Developmental Biology **245,** 329–347 (2002)
doi:10.1006/dbio.2002.0631, available online at http://www.idealibrary.com on IDEAL®

3D-DIASemb: A Computer-Assisted System for Reconstructing and Motion Analyzing in 4D Every Cell and Nucleus in a Developing Embryo

Paul J. Heid,[1] Edward Voss,[1] and David R. Soll[2]

W. M. Keck Dynamic Image Analysis Facility, Department of Biological Sciences, University of Iowa, Iowa City, Iowa 52242

A computer-assisted three-dimensional (3D) system, 3D-DIASemb, has been developed that allows reconstruction and motion analysis of cells and nuclei in a developing embryo. In the system, 75 optical sections through a live embryo are collected in the *z* axis by using differential interference contrast microscopy. Optical sections for one reconstruction are collected in a 2.5-s period, and this process is repeated every 5 s. The outer perimeter and nuclear perimeter of each cell in the embryo are outlined in each optical section, converted into *β*-spline models, and then used to construct 3D faceted images of the surface and nucleus of every cell in the developing embryo. Because all individual components of the embryo (i.e., each cell surface and each nuclear surface) are individually reconstructed, 3D-DIASemb allows isolation and analysis of (1) all or select nuclei in the absence of cell surfaces, (2) any single cell lineage, and (3) any single nuclear lineage through embryogenesis. Because all reconstructions represent mathematical models, 3D-DIASemb computes over 100 motility and dynamic morphology parameters for every cell, nucleus, or group of cells in the developing embryo at time intervals as short as 5 s. Finally, 3D-DIASemb reconstructs and motion analyzes cytoplasmic flow through the generation and analysis of "vector flow plots." To demonstrate the unique capabilities of this new technology, a *Caenorhabditis elegans* embryo is reconstructed and motion analyzed through the 28-cell stage. Although 3D-DIASemb was developed by using the *C. elegans* embryo as the experimental model, it can be applied to other embryonic systems. 3D-DIASemb therefore provides a new method for reconstructing and motion analyzing in 4D every cell and nucleus in a live, developing embryo, and should provide a powerful tool for assessing the effects of drugs, environmental perturbations, and mutations on the cellular and nuclear dynamics accompanying embryogenesis. **© 2002 Elsevier Science (USA)**

Key Words: **3D reconstruction; motion analysis; embryogenesis; *C. elegans*.**

INTRODUCTION

The patterns of a higher eucaryotic organism are laid down during embryogenesis. In this process, cell multiplication, cell differentiation, the definition of the body axes, cell and tissue reorganization, and the genesis of organ systems progress in an integrated fashion in time and space. With the advent of molecular and genetic tools, and sequencing of entire genomes, the regulatory mechanisms underlying the different aspects of embryogenesis are rapidly being elucidated. However, what is still lacking is a four-dimensional (4D) description of embryogenesis even in the simplest systems, such as *Caenorhabditis elegans*. A complete description would include 4D reconstruction and motion analysis of every cell cleavage, every nuclear division, every cell–cell interaction, and every change in cell shape through development of a single embryo. Such a description would provide us with insights into the spatial dynamics and cellular interactions basic to embryogenesis, and a context for evaluating the specific effects of mutations, environmental perturbation, and pharmacological agents on specific embryogenic processes.

To obtain such a description, a computer-assisted reconstruction and motion analysis system is essential. In recent years, a computer-assisted three-dimensional (3D) dynamic image analysis system (3D-DIAS) was developed for reconstructing at short time intervals the surface, nucleus, and pseudopods of living, crawling cells (Soll, 1995, 1999; Soll

[1] P.J.H. and E.V. contributed equally to this study.

[2] To whom correspondence should be addressed. Fax: (319) 335-2772. E-mail: david-soll@uiowa.edu.

0012-1606/02 $35.00
© 2002 Elsevier Science (USA)
All rights reserved.

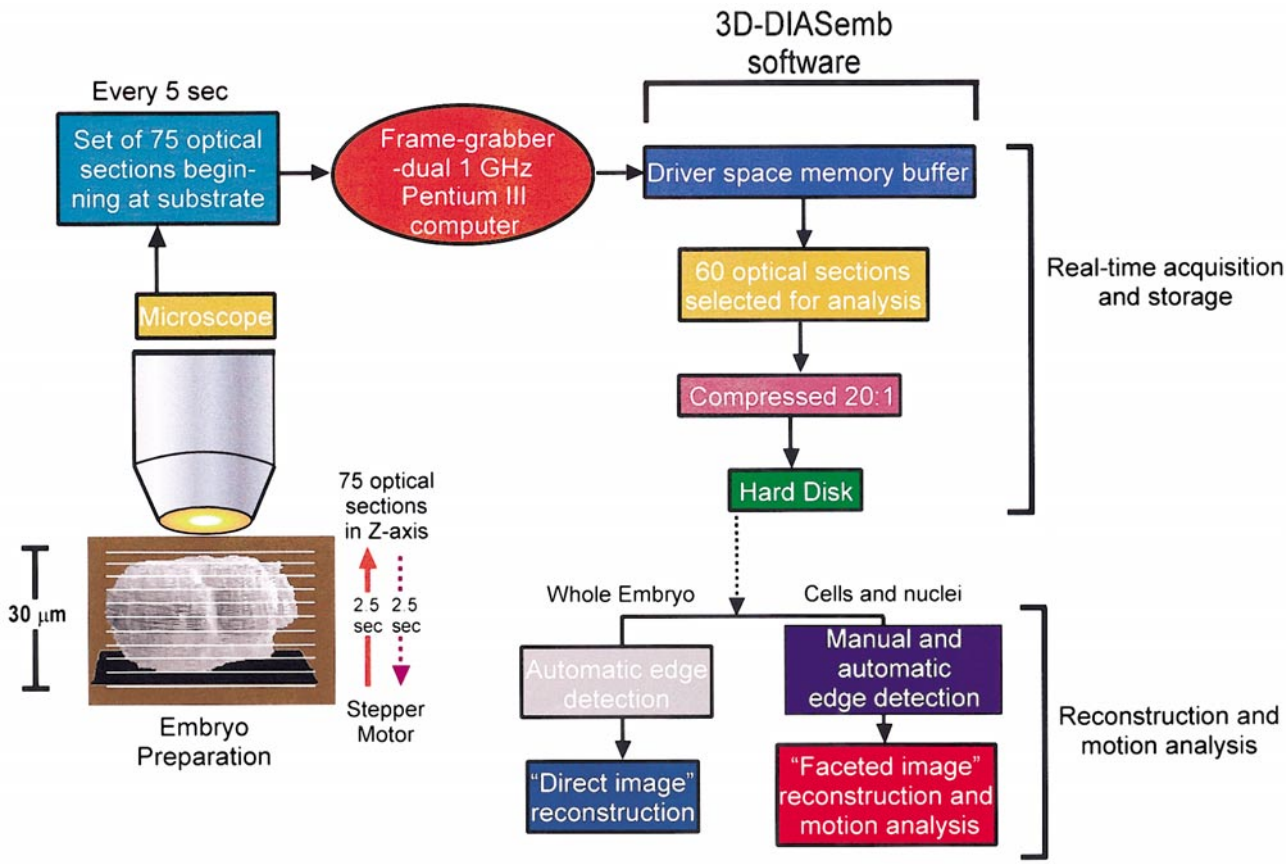

FIG. 1. The major components of "3D-DIASemb." A set of 75 optical sections through a developing embryo are acquired in a 5-s time interval through DIC optics. Optical sections are digitized into a memory buffer. Sixty sections are selected for analysis. The scan frames are compressed 20:1. Images are processed, and the edge of the entire embryo in each optical section is automatically outlined for "direct image reconstruction." In focus perimeters of each cell and nucleus are manually traced for faceted image reconstruction and motion analysis.

and Voss, 1998; Soll *et al.*, 2000; Wessels *et al.*, 1998). Using differential interference contrast (DIC) microscopy and computer-controlled stepper motors, a cell is optically sectioned in 1–2 s, and this process is repeated at intervals as short as 1–2 s (Wessels *et al.*, 1998). Using 3D-DIAS software, the edges of the cell, nucleus, and particulate-free zones of pseudopods in each optical section are digitized, the perimeters of each of these components converted to β-spline models, and the models used to generate faceted 3D reconstructions of a crawling cell. These reconstructions include the outer cell surface, the nucleus, and demarcated pseudopods, all color-coded for easy 3D discrimination. The time sequence of 3D reconstructions is then converted into an animated 3D computer movie that can be viewed from any angle through a stereo workstation. More importantly, every component of the dynamic 3D image (cell surface, cell centroid, pseudopod, and nucleus) can be individually motion analyzed, leading to quantitative phenotypes of wild-type and mutant cell behavior that have been instrumental in elucidating the roles of a number of cytoskeletal and regulatory elements in motility and chemotaxis (Wessels and Soll, 1998; Shutt *et al.*, 1995; Wong *et al.*, 2000; Wessels *et al.*, 2000a,b; Tuxworth *et al.*, 2001; Stites *et al.*,1998). Although the first effective computer-assisted 3D reconstruction and motion analysis system (3D-DIAS) for individual cells was developed several years ago (Soll, 1995; Wessels *et al.*, 1998; Shutt *et al.*, 1995; Murray *et al.*, 1992), the application of this technology to embryogenesis first required software that would individualize every cell and its progeny over time, and every nucleus and its progeny over time, then reassemble them into a dynamic 3D model of the developing embryo.

Recently, we expanded the computing power of 3D-DIAS and developed the necessary software for processing, accessing, reconstructing, and motion-analyzing every cell and nucleus in a developing embryo. In developing this system, we employed the *C. elegans* embryo as our experimental model. Using a customized computer-regulated motor for

© 2002 Elsevier Science (USA). All rights reserved.

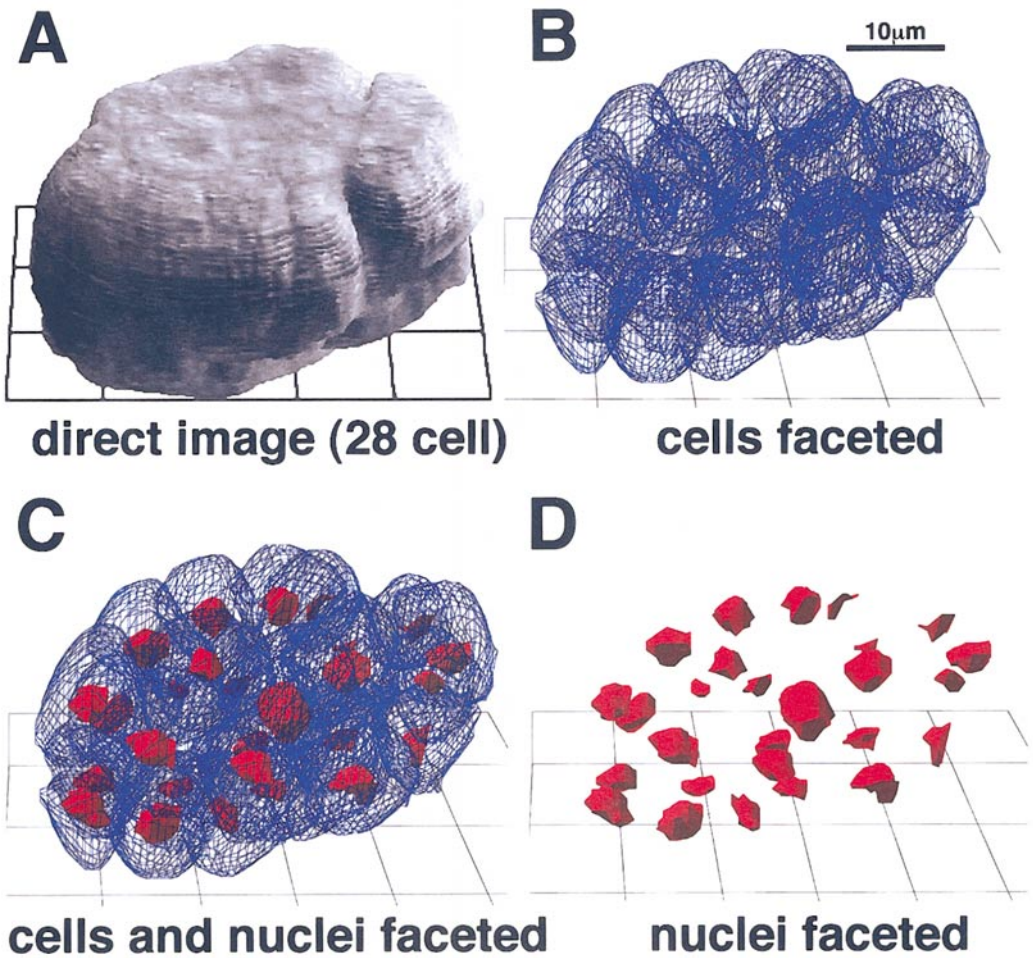

FIG. 2. The four major 3D-DIAS embryo presentations are (A) the "direct image reconstruction," in which the automatically interpreted perimeter of the embryo image in each optical section is filled with the original DIC image and stacked, (B) the transparent "faceted reconstruction" of the 3D surface of all cells in the embryo, (C) the image in (B) to which is added the nontransparent faceted reconstructions of nuclei, and (D) the nuclei alone.

optically sectioning embryos, DIC optics, and newly developed 3D-DIAS software, which we have named "3D-DIASemb" for "3D-DIASembryo," 75 optical sections are collected through the *z* axis of a live, developing embryo in a 2.5-s period, and the process is repeated at 5-s intervals (Fig. 1). The edge of each cell and nucleus is traced in individual trace slots, the perimeters converted into β-spline models, and from the individual stacks of modeled perimeters, each cell and each nucleus in the developing embryo is reconstructed as a faceted image in 3D at intervals as short as every 5 s. At each time point, the models of all cells and nuclei are merged into a 3D model of the entire embryo. The sequence of reconstructions of the single developing embryo can then be viewed as a 3D movie through a stereo workstation. 3D-DIASemb allows one to view for the first time the developing embryo from any angle through time and space, to isolate and follow in time any cell and subsequent progeny (cell lineage), to subtract cell surfaces and follow all nuclei, or one nucleus and progeny nuclei (nuclear lineage), in time. Since the surfaces of each cell and each nucleus have been converted to β-spline models, 3D-DIASemb provides more than 100 parameters of motility and dynamic morphology for each cell and nucleus at time intervals as short as 5 s. Finally, the system provides "direct image reconstructions" that can be analyzed for particle movements within the cytoplasm, generating vector flow plots of cytoplasmic flow. Here, we describe for the first time this new system as it is applied to early *C. elegans* embryogenesis. 3D-DIASemb provides researchers for the first time the capability of reconstructing and motion analyzing the behavioral dynamics of every cell and nucleus in a developing embryo. This new system should be especially valuable in quantitatively assessing the effects of drugs, environmental perturbations, and mu-

© 2002 Elsevier Science (USA). All rights reserved.

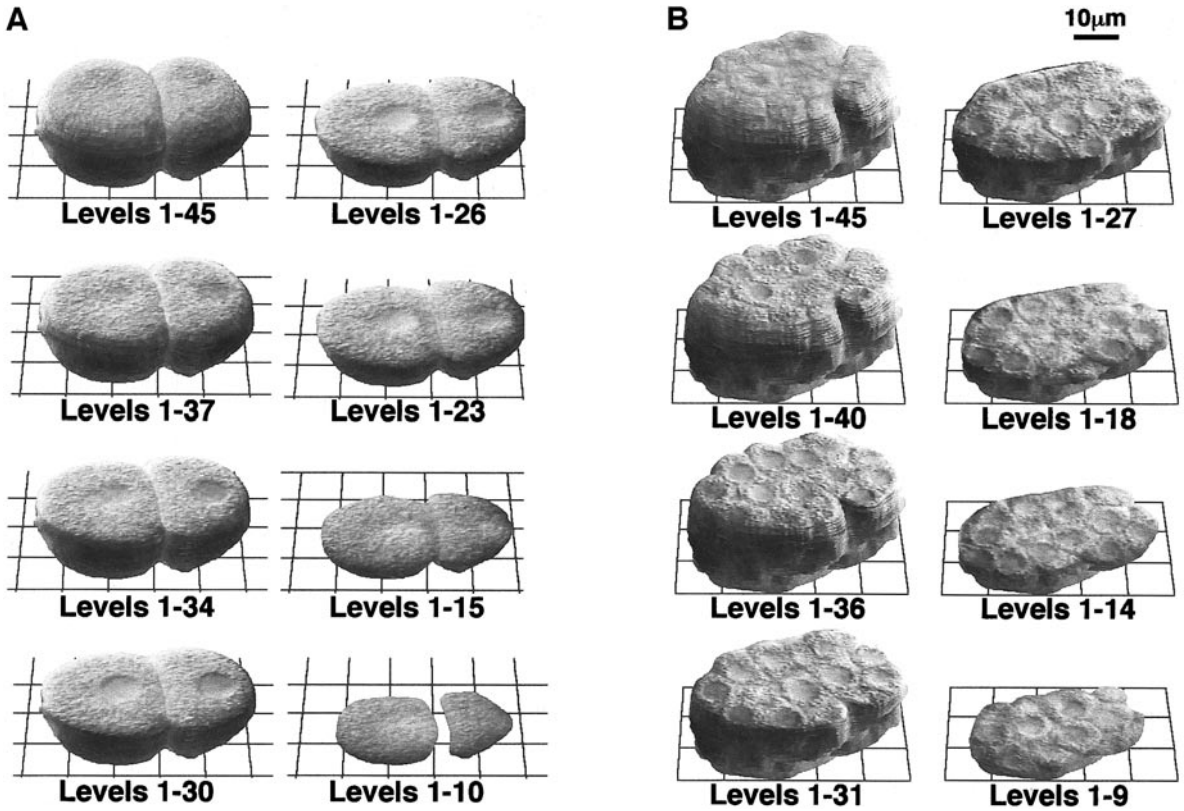

FIG. 3. Progressively stacked optical sections processed for direct image reconstruction of a developing embryo at the 2- (A) and 28-cell (B) stages. Once stacked, the direct image reconstruction can be accessed at any level. Computer movies can be generated at any level through development, with time intervals between images as short as 5 s.

tations on the behavior of individual cells and nuclei accompanying embryogenesis.

METHODS AND RESULTS

Preparation of C. elegans embryos. Embryos of the *C. elegans* Bristol strain N2 were cultured at room temperature (21°C) as previously described (Brenner, 1974). This strain was obtained from the *C. elegans* Genetic Stock Center at the University of Minnesota (Minneapolis, MN). Embryos were obtained by placing gravid hermaphroditic animals in depression wells in a glass slide filled with M9 buffer (Sulston *et al.*, 1983). Animals were bisected transversely at the vulva, releasing embryos into the buffer. Embryos were individually transferred to a slide covered with a thin film of 0.5% agar. Individual embryos were brushed from the initial pool of liquid to the center of the agar pad with an eyelash, and allowed to settle. A drop of M9 buffer was distributed over the embryos, and a coverslip was placed over the preparation. Excess agar was trimmed from the edges of the pad with a razor blade, and the edges of the coverslip were sealed to prevent dehydration (Sulston and Horvitz, 1977). Alternatively, embryos were mounted on poly-L-lysine-coated coverslips, which were then placed on a slide with two pieces of laboratory tape along the edges of the coverslip to act as spacers to avoid pressure on the embryos by the overlying coverslip.

Optical sectioning and image acquisition. A diagram of 3D-DIASemb is presented in Fig. 1. Embryos were imaged through a 63× oil immersion objective (NA 1.4) of a Zeiss ICM405 inverted microscope equipped with DIC optics. The shaft of the coarse focus knob was attached to an Empire Magnetics (Rohret, CA) IN-23P stepping motor controlled by a New England Technologies (Lawrence, MA) NEAT 101M motor driver. This system provided 44 steps per micron, which was more than adequate. The motor was controlled by a custom-designed Linux driver using the parallel port of a 833 MHz Pentium III processor-equipped computer. For added torque, a high precision motor gear box with a 1:4 step down ratio was utilized, allowing the motor to operate at 4000 steps per second, and move through 90 μm in 1 s. In optically sectioning embryos, the stepper motor moved the stage a total of 30 μm in 2.5 s in each direction. A Burst Electronics (Corrales, NM) MCG-2 micro character generator was inserted in the video path. It was

© 2002 Elsevier Science (USA). All rights reserved.

controlled via the serial port by the Linux driver to mark each video frame for the direction of movement (up vs down), in order to synchronize the beginning of each scan. In reconstructing embryos, only the optical sections in the upscans, collected in 2.5 s and repeated at 5-s intervals, were used (Fig. 1). This provided 75 sections, beginning below the substrate, and ending above the embryo. Only the middle 60 sections, beginning at the substratum, were used for reconstruction, with the additional 15 sections providing room to bracket the lowest and highest points of the embryo.

To acquire optical sections in the upscans, a Data Translation (Marlborough, MA) DT3152 frame grabber running on a custom-built dual 1 GHz Pentium III computer with Windows 2000 was programmed. As the scan progressed upward, the 75 video frames were frame-grabbed into a special driver-space memory buffer. As the scan progressed downward, the 75 upscan frames were transferred to regular computer memory and compressed 20:1 at a rate of 30 frames per second by using our own version of the Discrete Cosine Transform (DCT) combined with modified Golumb coding (Saloman, 1998). This version achieved a better compression ratio than the standard JPEG method because grayscales rather than colors were used, and because the DCT frequency filters were adjusted for DIC optics. The dual processors divided this task so that each compressed only 15 frames per second. Compression is performed during the 2.5-s downscan. Processor 1 grabbed 75 frames, while processor 2 transferred the previously compressed 75 frames to the hard disk (100 ATA IBM Desk-star, 30 Gbyte), providing real-time acquisition and storage of upscan sections. With compression, 1 h of recording used 690 Mbyte of memory, and 6 h of recording could be stored on six standard 700-Mbyte CDs. The original 3D-DIAS program was modified to allow the compressed DCT format files to be transferred to a Macintosh 450 MHz G4 computer.

Modification of 3D-DIAS in the development of 3D-DIASemb. Two major hurdles were overcome in converting the original 3D-DIAS program to 3D-DIASemb. First, the number of trace slots had to be increased to accommodate the increasing number of cells and nuclei in a developing embryo. The original 3D-DIAS program had 10 functioning trace slots. It was designed by using "short" 16-bit integers. On the Macintosh, each file has an attached mini-database called the resource fork. Resource forks allow a maximum of 2727 entries and have a maximum size of 16 Mbyte. To increase the number of trace slots to 10,000, a scheme was employed in which 1024 traces at a time were compressed and bundled into each resource fork entry, and all "short" 16-bit short integers were converted to "long" 32-bit integers. One hour of an embryo recording, in which 60 optical sections are collected every 5 s, resulted in 43,200 optical sections. Next, the video file had to be compressed. An hour of uncompressed embryo recording required 8 Gbyte of hard disk space, well above the 2 Gbyte limit per file. QuickTime offered good compression but slow access to single frames in 3D-DIAS. Therefore, a compression scheme was designed based on the DCT that achieved 20:1 compression. The DCT frequency filters were fine-tuned to maximize image quality of the DIC images. The dual 1-GHz Pentium III processor-equipped PC with a frame grabber was used to acquire optical sections. This allowed 1 h of video to fit on a single CD-ROM. Finally, the original 3D-DIAS program was modified to handle the vastly increased number of trace slots and movie frames, the 3D viewer was modified for multicellular complexes, and new algorithms were written for fast playback of complex faceted images that were compatible with the CrystalEyes 3D stereo viewing system (Stereographics, San Raphael, CA).

Outlining cell perimeters and nuclei for reconstructions. 3D-DIASemb produces five kinds of embryo reconstructions: a "direct image" reconstruction (Fig. 2A), a transparent faceted image reconstruction of cell surfaces alone (Fig. 2B), a nontransparent faceted image reconstruction of cell surfaces (not shown, see Figs. 9C and 9D), a transparent faceted image reconstruction of cell surfaces with nontransparent nuclei (Fig. 2C), and nontransparent reconstruction of nuclei alone (Fig. 2D). As noted, these reconstructions can be generated every 5 s during embryogenesis, can be made into a continuous movie, and can be viewed from any angle. The latter three reconstructions (Figs. 2B–2D) depend on outlining the in-focus perimeter of every cell and nucleus in each optical section. For the 3D reconstruction of independent cells (i.e., cells not touching other cells), the 3D-DIAS program provides a number of different algorithms for automatic edge detection (Soll and Voss, 1998; Soll, 1999; Soll *et al.*, 2000; Wessels *et al.*, 1998). Although none of these algorithms are at present sufficient for defining the edges of cells contacting other cells in DIC images of embryos, the "pixel complexity transform" can be used to detect automatically the outer edge of the entire embryo in every optical section for direct image reconstructions, as in Fig. 2A. This general procedure for edge detection has been described in detail in a previous publication (Soll *et al.*, 2000). In brief, a custom transform is used in which the intensity of each point in the image is converted to the standard deviation of the pixel values within a kernel centered at that point (Soll *et al.*, 2000). This conversion generates hundreds of regions, which are fused by "dilation," then reduced to the original size by "erosion," providing a single encapsulated, outlined perimeter. Methods are then applied to optimize the outlines and remove noncellular detail. The result of this process is a stack of approximately 60 2D perimeters filled with the original DIC images. The process stacks the optical sections from bottom to top, each section hiding the section below (Figs. 3A and 3B). The regions separating the boundaries where the upper slice lies upon a lower slice are jagged (i.e., "aliased"). To improve image quality, rays are traced form the virtual eye position to the stacked image at a 4:1 subpixel density with bi-cubic interpolation providing extra pixel density, a means of "anti-aliasing." Since ray tracing is time consuming (Watt, 1993), we developed software for

© 2002 Elsevier Science (USA). All rights reserved.

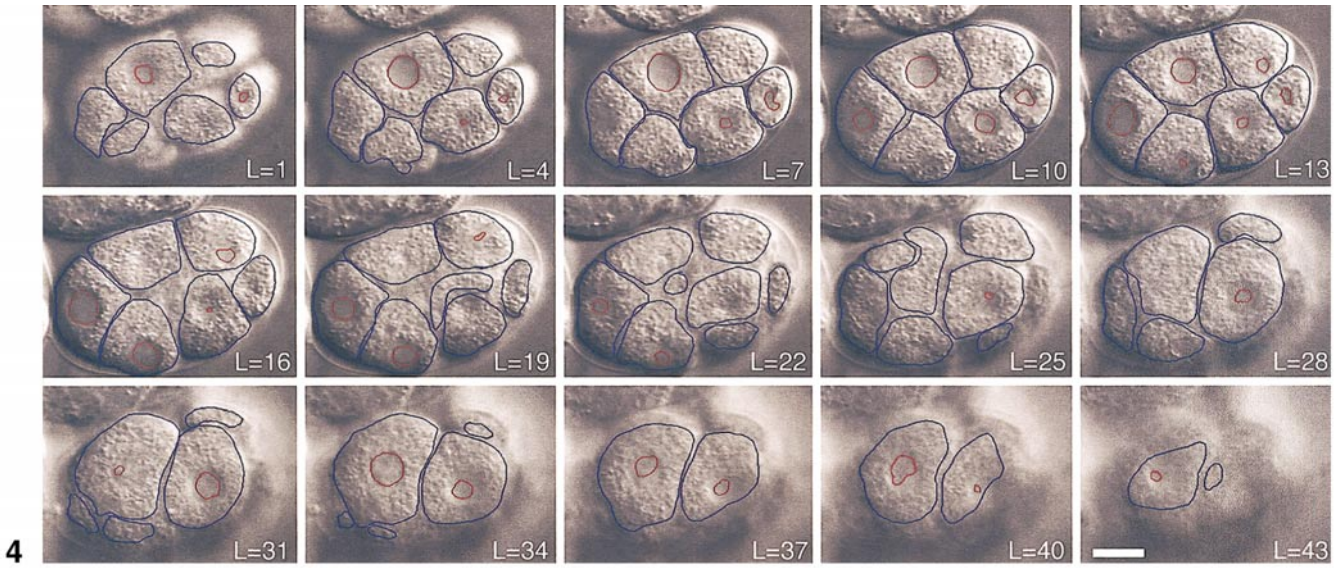

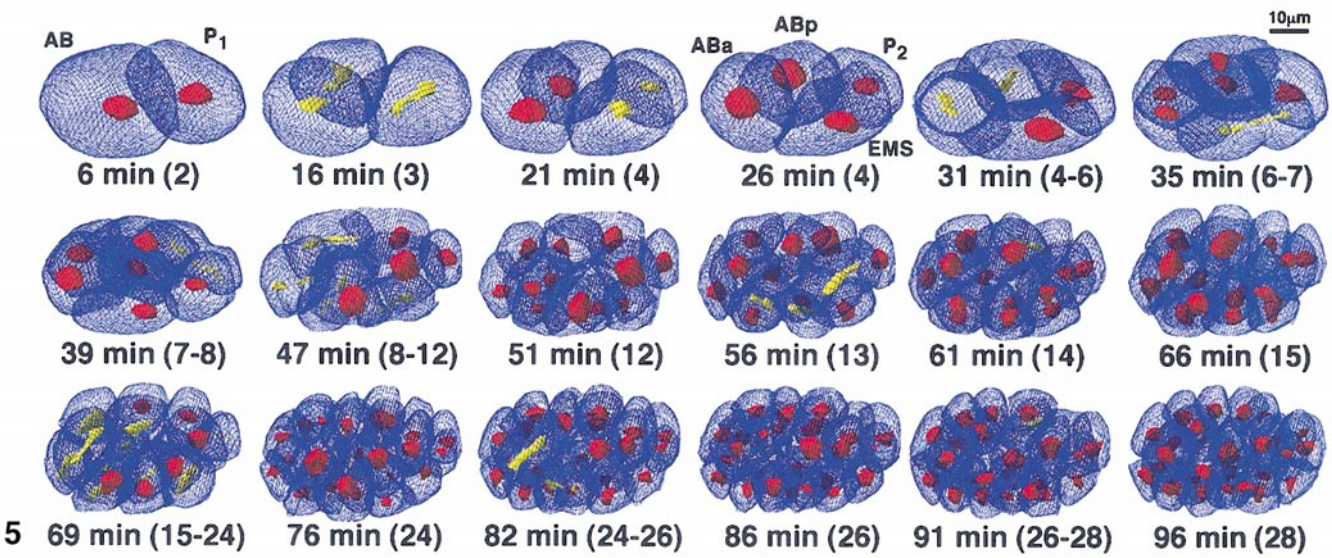

FIG. 4. Tracings of the in-focus edges of cells (blue) and nuclei (red) of an 8-cell embryo at select levels (L) of the 60 optical sections collected at one time point. These perimeters are then converted to β-spline models and stacked. The stacks of each cell and nucleus are then converted into a faceted image (Fig. 2C). Scale bar, 10 μm.

FIG. 5. Faceted reconstructions of the developing *C. elegans* embryo from the 2- to 28-cell stage. Cell surfaces are presented as transparent blue faceted images, interphase nuclei as nontransparent red faceted images, and mitosing nuclei as nontransparent yellow faceted images. Time is presented in minutes (min) with cell number in parentheses at the bottom of each reconstruction.

tracing in reverse, from the image to the eye, using large (50 Mbyte RAM) look-up tables to reduce the number of computations for each projection. In Figs. 3A and 3B, the progressively stacked optical sections of a 2- and 28-cell embryo, respectively, are presented. Once the complete set of sections is stacked, it can be accessed at any depth, and movies can be made of the changes over time at any particular depth or at any angle in the embryo.

Although direct image reconstructions are informative, especially when accessed at different depths, and, as shall be discussed, provide information on cytoplasmic flow, they are not in a form readily amenable to the computation of motion analysis parameters. For that purpose, the stacked perimeters of the cell and nucleus must be converted to faceted 3D models. To generate a faceted model of the embryo at each time point, the in-focus perimeter of every cell and nucleus was manually outlined in each optical section. Our main objective in software develop-

© 2002 Elsevier Science (USA). All rights reserved.

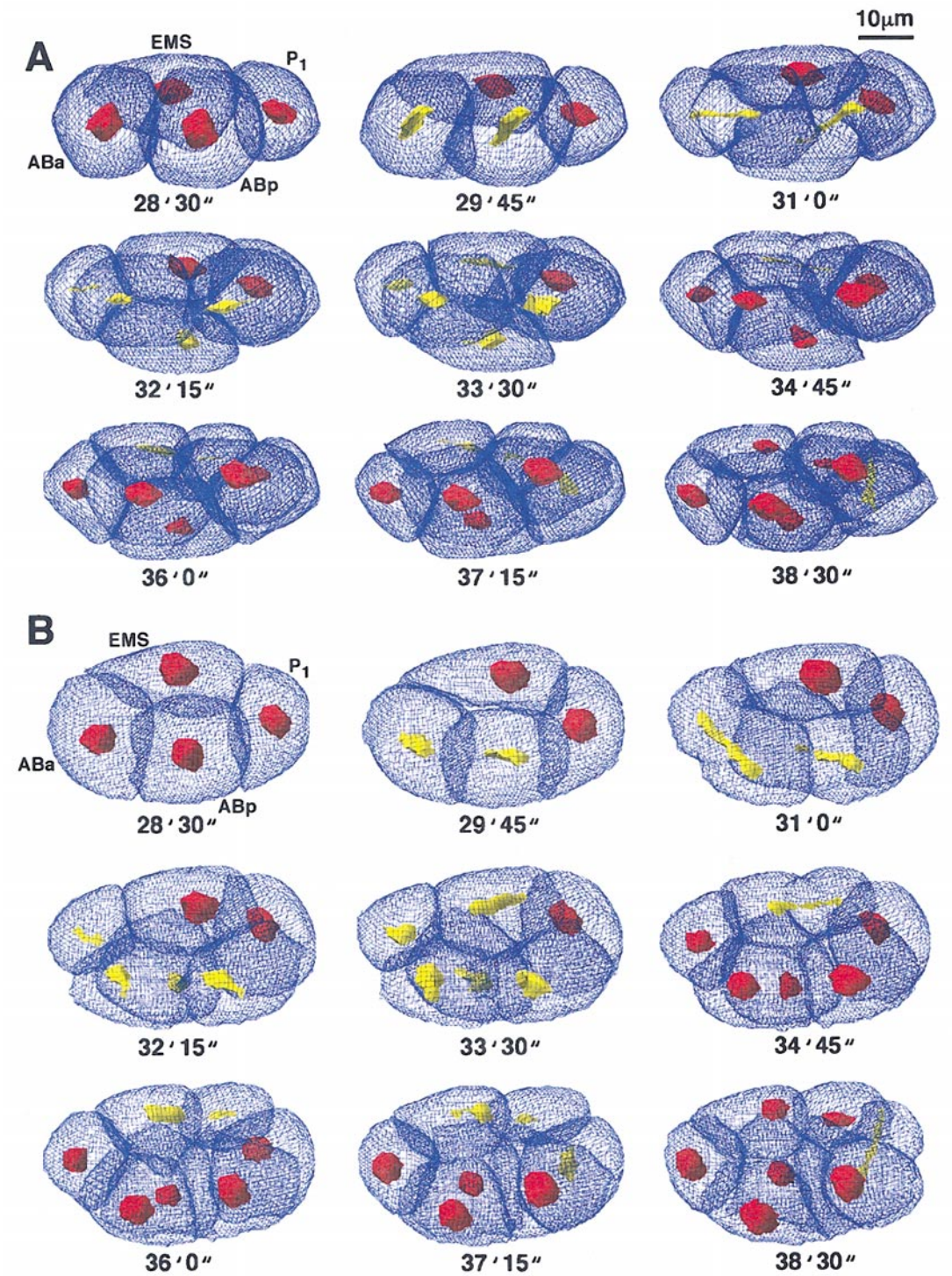

FIG. 6. 3D-DIASemb reconstruction of a developing embryo at 15-s intervals between the four- and eight-cell stages. Cell surfaces are presented as blue faceted images, interphase nuclei as nontransparent red faceted images, and mitosing nuclei as nontransparent yellow faceted images. The view in (A) is at a 20° angle, and the view in (B) at a 70° angle. The initial cell types are noted at 28′30″.

© 2002 Elsevier Science (USA). All rights reserved.

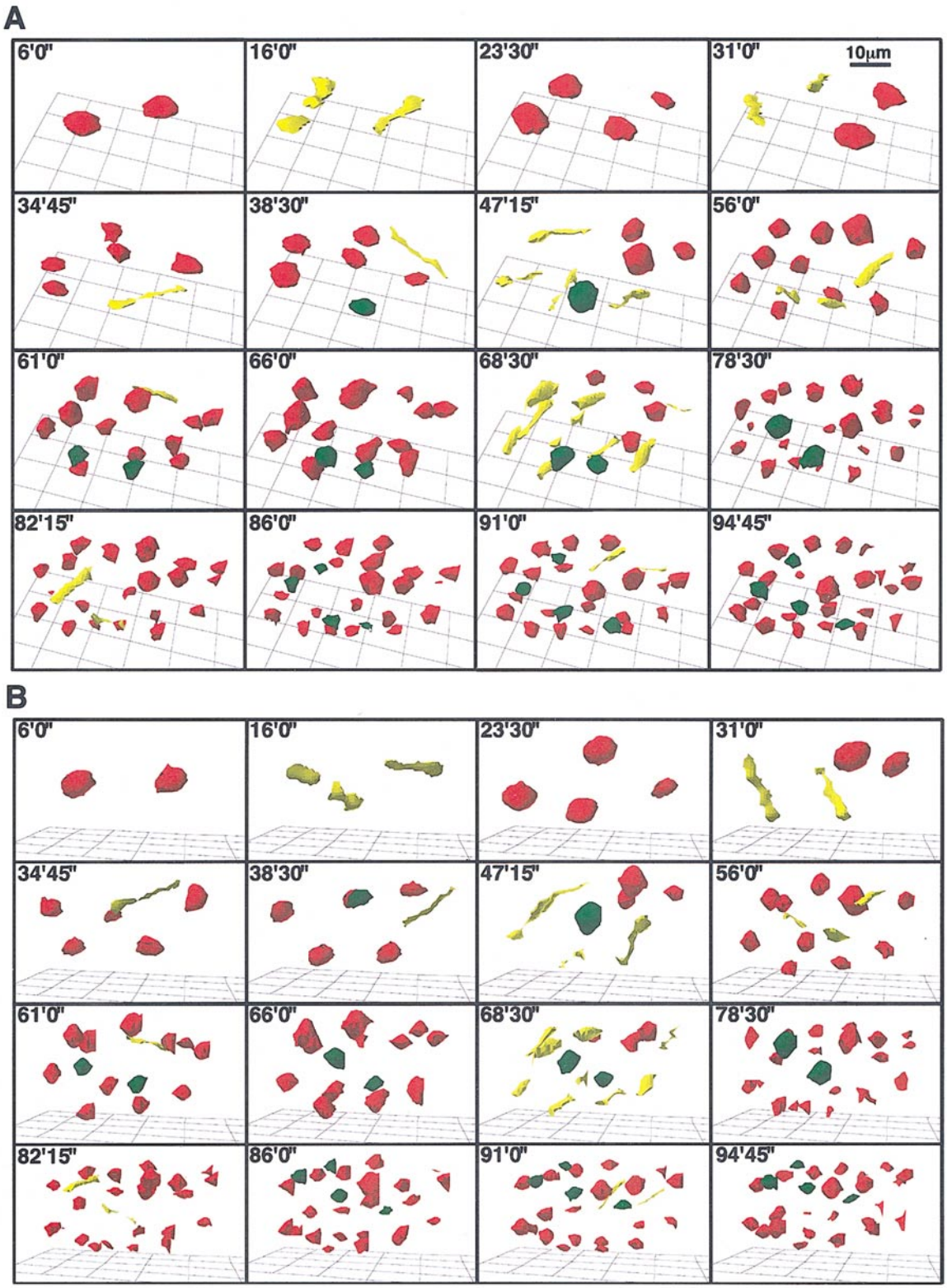

FIG. 7. 3D-DIASemb allows reconstruction of nuclei alone. The view in (A) is at a 45° angle, and in (B) at a 10° angle (see grid for reference). Interphase nuclei are color-coded red, mitosing nuclei yellow, and MS-derived nuclei green. When MS-derived nuclei undergo mitosis, they are also color-coded yellow.

© 2002 Elsevier Science (USA). All rights reserved.

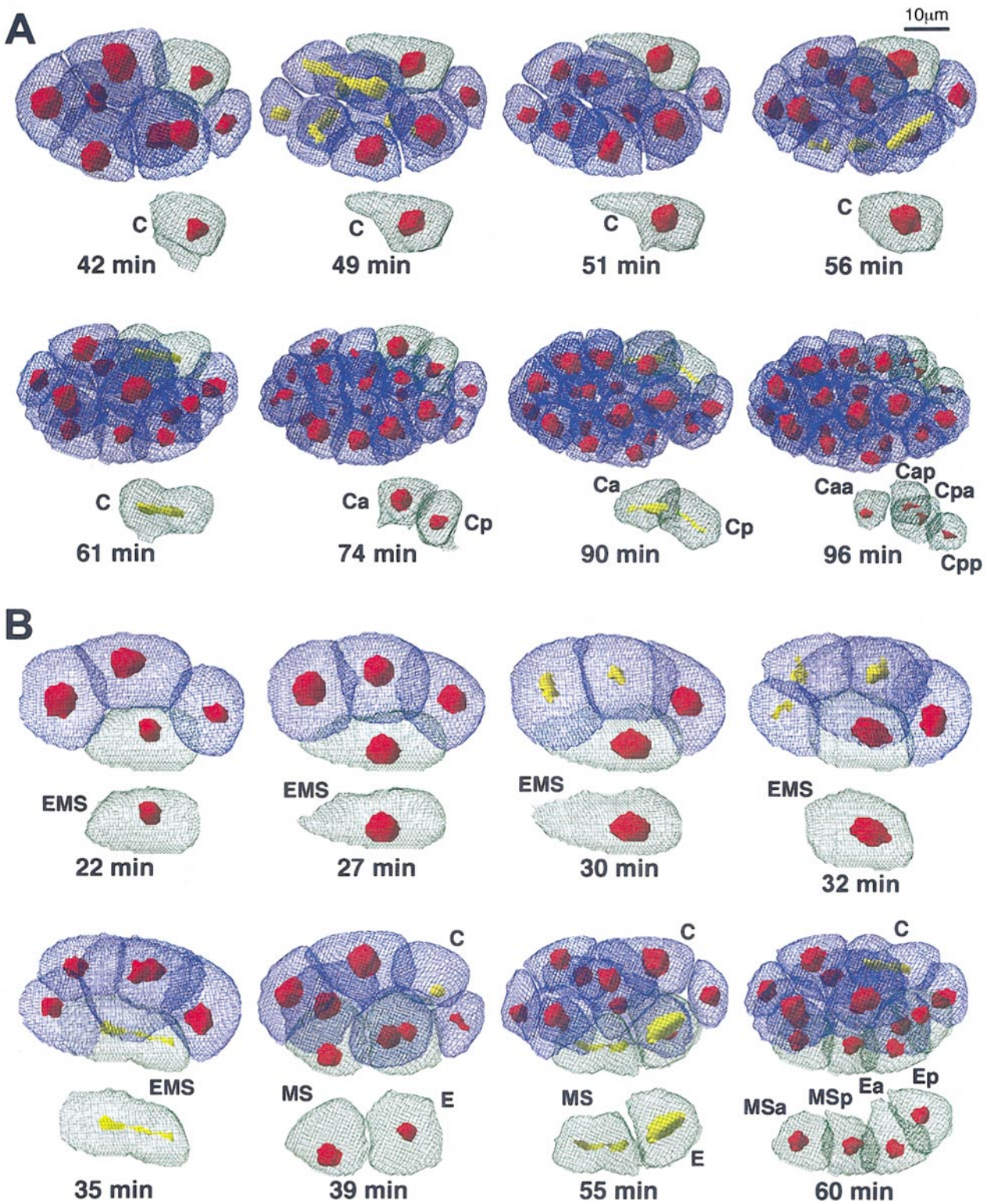

FIG. 8. 3D-DIASemb allows isolation and analysis of cell lineages. Examples are presented of cells that undergo cell shape changes during early embryogenesis. (A) The C cell and its descendants are followed from the 8-cell through the 28-cell stage. (B) The EMS cell and its descendants are followed from the 4-cell through the 14-cell stage. The isolated cells are color-coded green, other cells are color-coded blue, interphase nuclei are color-coded red, and mitosing nuclei are color-coded yellow. The C cell extends an arm around neighboring AB cells as the latter divide between 49 and 51 min. The EMS cell extends an arm around the ABa cell in the 4-cell embryo between 27 and 30 min.

© 2002 Elsevier Science (USA). All rights reserved.

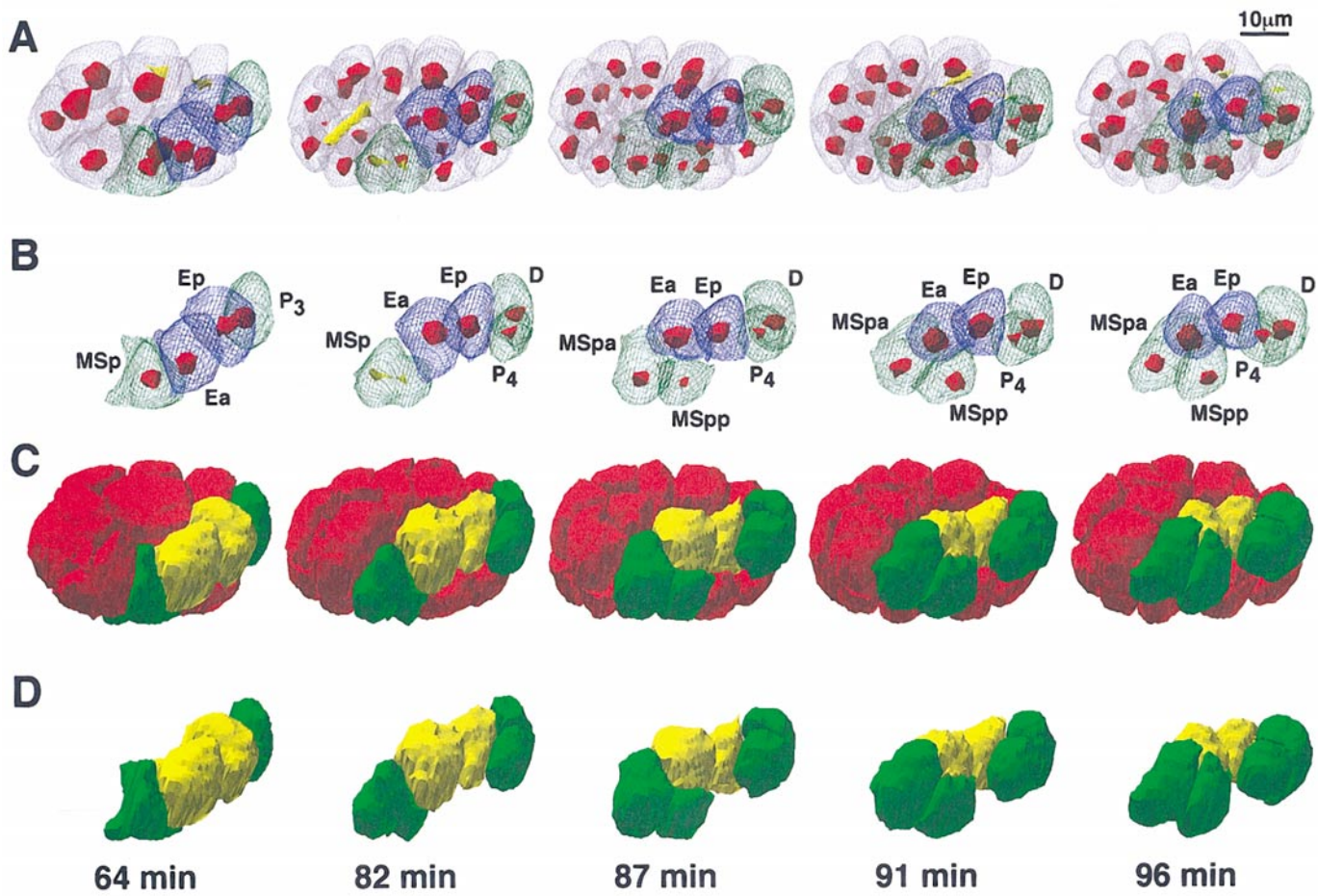

FIG. 9. 3D-DIASemb allows isolation of a group of cells, in this case the cells involved in gastrulation. (A, B) Transparent faceted images with nuclei. The two E cells, the first to invaginate during gastrulation, are color-coded blue, and the cells that move over the E cells, MSp and its progeny MSpa and MSpp, and P_3 and its progeny P_4 and D, are color-coded green. All other cells in the embryo are color-coded gray. (C, D) Nontransparent faceted images. The two E cells are color-coded yellow, MSp and progeny and P_3 and progeny are color-coded green, and all other cells are color-coded red.

ment at this moment is to automate this process (see Discussion), as we have done for individual crawling cells and the left ventricle of a beating heart imaged by ultrasound (Soll, 1999; Soll *et al.*, 2000; Wessels *et al.*, 1998). For the time being, features have been added to 3D-DIASemb to facilitate manual outlining and editing. In Fig. 4, traces are shown of an eight-cell embryo at representative positions through the *z* axis series. Traces of cell perimeters are blue and traces of nuclear perimeters are red. In both cases, the interface between in-focus and out-of-focus regions is traced. "Shadows" at these interfaces caused by out-of-focus steep edges help define the interfaces. Interpreted interfaces of cells do not always abut adjacent cells, suggesting that spaces exist between cells, especially near the center of the embryo (e.g., L = 19; Fig. 4). Comparisons of the original unprocessed images, image-processed optical sections, and outlined images suggested that the larger central spaces were extracellular cavities, while narrow spaces between cells were artifactual. Experiments employing vital membrane stains and live laser scanning confocal microscopy are now in progress to define true spaces between blastomeres. Perimeters of nuclei were also identified as the outer edge of the in-focus portion of the image. During periods of nuclear envelope breakdown, the nuclear region was traced as the granule-free region of cytoplasm within the dividing cell.

Generating faceted 3D reconstructions of cells and nuclei. The continuous perimeter encompassing each cell image in an optical section was converted to a β-spline representation (Barsky, 1988). The β-spline representations were then stacked, generating a 3D contour map. One triangulated net was then projected over the top (top down) of the contours and a second triangulated net was projected in the reverse direction (bottom up) over the bottom of the

© 2002 Elsevier Science (USA). All rights reserved.

contours. The nets were trimmed at their junctions and joined by intersecting triangular sections in the intervening space. The methods for determining top and bottom nets, for mapping triangles upward, and for filling junction spaces have been described for the reconstruction of single cells (Soll *et al.*, 2000). The same method was used to reconstruct each nucleus in the developing embryo. The resulting facets of each reconstruction were individually stored in a facet database file. Up to 10,000 individual faceted components could be stored for each reconstruction. Information about each cell and nucleus was stored in the resource fork of the facet file. This information included parent, progeny, view angle, color code, etc. Once the faceted image of each cell in an embryo was generated at a specific time point, the cell reconstructions could be merged to generate the image in Fig. 2B. Once the faceted images of the nuclei in an embryo were generated at a specific time point, they could be merged with the cell surface images to generate the image in Fig. 2C.

Reconstructing the C. elegans embryo from the 2- to 28-cell stage. In Fig. 5, a developing *C. elegans* embryo has been reconstructed at approximately 5-min intervals from the 2- to 28-cell stage. The faceted surfaces of cells are presented as transparent blue caged images, the faceted surfaces of nuclei are presented as nontransparent red images, and the faceted surfaces of nuclei undergoing mitosis are presented as nontransparent yellow images (Fig. 5). This reconstruction format provides one with a view of cell shape changes over time, cell–cell relationships in space and time, asynchronous and synchronous nuclear divisions, and the spatial orientation of every nuclear division. As previously demonstrated by Sulston *et al.* (1983), one can readily identify synchronous division of ABa and ABp (Fig. 5, 31 min) and the subsequent division synchrony of cells in the AB founder cell lineage (Fig. 5, 47 min). All times in all figures are presented as minutes after first cleavage. Asynchronous division of AB and P_1 is obvious between 6 and 21 min. Additional asynchronous and synchronous divisions are obvious through the 28-cell stage (Fig. 5). Because one can rotate each reconstruction, one can also map the exact plane of mitosis, and changes in cell position and cell–cell contacts at each stage. One can also select any period and generate reconstructions at far shorter time intervals. For example, in Fig. 6, reconstructions are presented at 1′15″ time intervals between the 4- and 8-cell stages. Such reconstructions can be viewed at different angles (e.g., at 20 degrees in Fig. 6A and at 70 degrees in Fig. 6B), providing greater spatial and temporal resolution for the identification of rapid events. In Fig. 6A, one can see that the angles of the mitotic apparatus of ABa and ABp are nearly identical at 29′45″. However, the angles of the mitotic apparatus of ABa and ABp diverged between 29′45″ and 31′0″. Finally, one can generate a movie at any angle which facilitates identifying spatial and temporal differences.

Reconstructing nuclei only. The 3D-DIASemb program provides the option of subtracting all cell surfaces, leaving in place only cell nuclei (Fig. 7). This affords one with a less obstructed view of the temporal and spatial dynamics of nuclear division, and the changes that occur in nuclear shape and volume. It should be noted that because of the long interval time between reconstructions, many of the mitoses were missed in the sequence in Fig. 5, and because of the very short time intervals in Fig. 6, only one set of nuclear divisions is described. In Fig. 7, times were selected that included most mitoses between the 2- and 28-cell stages. In addition, the MS cell nucleus is color-coded green at 38′30″ (the 7-cell stage), and subsequent progeny of the MS cell nucleus also color-coded green, except at the time of mitosis (yellow), through the 28-cell stage. 3D-DIASemb allows one to perform this for any nuclear lineage at any time during embryogenesis. Alternatively, one can subtract all nuclei other than the nuclear lineage of interest through a time series (data not shown).

Reconstructing a single cell lineage. Because every cell and every nucleus are individually reconstructed in space and time, 3D-DIASemb provides the capability of isolating and following any individual cell lineage. Such isolation can reveal specific changes in cell morphology that may play fundamental roles in embryogenesis. In Fig. 8A, reconstructions of the complete embryo, including cell surfaces and nuclei, are presented in which the C cell lineage is color-coded green and hence distinguished from other cells color-coded blue, from the 8-cell stage (42 min) to 28-cell stage (96 min). Reconstructions demonstrated that the C cell at the 8-cell stage extended an arm around the ABpl cell while the latter was dividing (Fig. 8A, 49 min). This extension was then retracted between 51 and 56 min, 5 min prior to the first C cell division (Fig. 8A). The C cell progeny Ca and Cp then divided synchronously at 90 min (Fig. 8A). In a second embryo analyzed in the same manner, the same C cell extension was observed at approximately 49–51 min (data not shown). To be sure that this was not a cell type-specific artifact due to the compression caused by the coverslip, we monitored C cell morphology in an embryo mounted in a chamber with a spacer that prevented compression of the embryo by the coverslip, and observed similar C cell extension at approximately 49 min (data not shown).

In Fig. 8B, a second example is presented of a cell that undergoes a shape change, in this case the EMS cell. The EMS cell formed an extension between 22 and 30 min, then retracted the extension between 30 and 32 min (Fig. 8B). The EMS cell then divided into the MS and E cells 3 min later. The MS and E cells in turn divided at approximately 55 min (Fig. 8B). Reconstructions at half-minute intervals revealed that the MS and E cells divided 1 min apart, at 55 and 56 min, respectively (data not shown). The extension of the EMS cell was also verified in a noncompressed embryo (data not shown). The ability to isolate individual cells and follow the changes in cell morphology and subsequent nuclear divisions sometimes unmasks behavior camouflaged by neighboring cells in a composite reconstruction.

Reconstructing gastrulation. Because cells are individually digitized, 3D-DIASemb provides the capability of

© 2002 Elsevier Science (USA). All rights reserved.

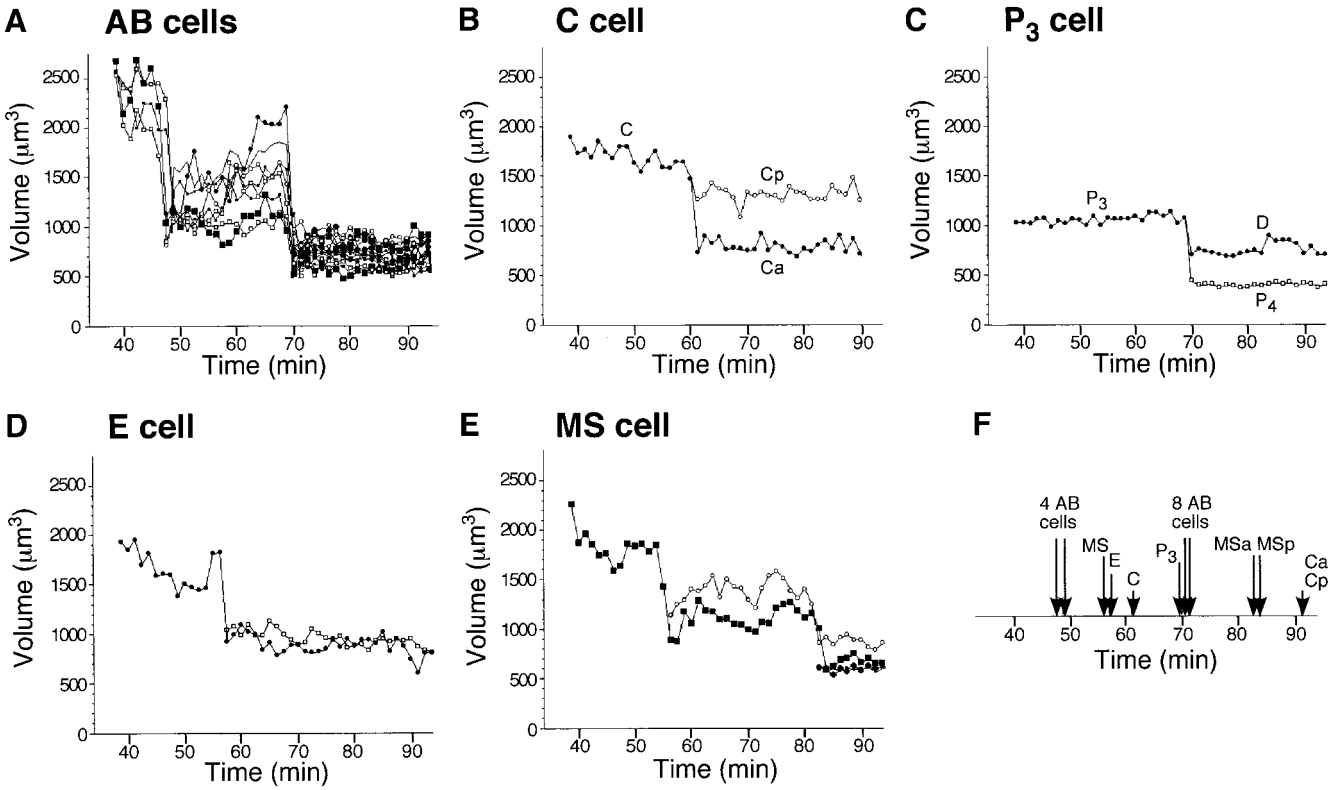

FIG. 10. 3D-DIASemb provides time plots of motility and morphology parameters for individual cells and progeny, in this case cellular volume (A–E). From these plots, one can accurately assess the exact times of cytokinesis (F) and distinguish between symmetric and asymmetric divisions. The two arrows for the 4AB and 8AB cells indicate a small range of cell division times in each case.

isolating and following the cellular interactions within a selected group of cells. In Fig. 9A, the cells that play a major role in the initial movements during gastrulation are color-coded blue and green in transparent faceted reconstructions that include nuclei. It is clear that reorganization of these cells occurs between 64 and 96 min, but it is difficult to resolve these changes in the composite reconstruction of transparent faceted cells in the embryo (Fig. 9A), even with color-coding. Therefore, the group of cells involved in this reorganization (progeny of MSp, E, and P_3) has been isolated and monitored over the same time period (Fig. 9B). This presentation not only allows one to follow more readily the ingression of Ea and Ep (the blue cells) and the enveloping behavior of MSp and P_3 (the green cells), but also the nuclear and cell divisions of MSp and P_3 accompanying these embryogenic movements. Because the behavior of an isolated subgroup of transparent faceted cell images can sometimes be difficult to interpret in space, one can generate nontransparent images of the whole embryo, in which the cells of interest are color-coded (Fig. 9C), or nontransparent images of the isolated cells of interest (Fig. 9D). These latter reconstructions provide a more vivid display of ingression during early gastrulation.

Quantitating the embryonic, cellular, and nuclear changes during embryogenesis. Because each cell and nucleus is individually reconstructed, then reassembled, each cell and nucleus can be individually motion-analyzed, using 3D-DIASemb software to compute roughly 100 individual parameters, based on centroid dynamics and changes in contour (Soll, 1995; Soll and Voss 1998). With use, 3D-DIASemb will acquire new parameters that are specific to the changes accompanying embryogenesis, most notably those that assess multicellular interactions, and spatial and temporal relationships. Here, it suffices to demonstrate the power of 3D-DIASemb for quantitation using established single cell parameters. In Fig. 10, 3D-DIASemb software was used to compute the volumes of the AB, C, P_3, E, and MS cell lineages as a function of development time. In Fig. 10A, the volumes of the four AB progeny, beginning at 38 min after the first cleavage, are monitored through two subsequent divisions. It is clear from these plots that the 4 AB cells divided relatively synchronously at approximately 48 min and that the 8 progeny cells divided relatively synchronously at approximately 69 min. In each case, there was a 1-min difference in some AB lineage divisions. The volumes of the original four AB cells were distributed

© 2002 Elsevier Science (USA). All rights reserved.

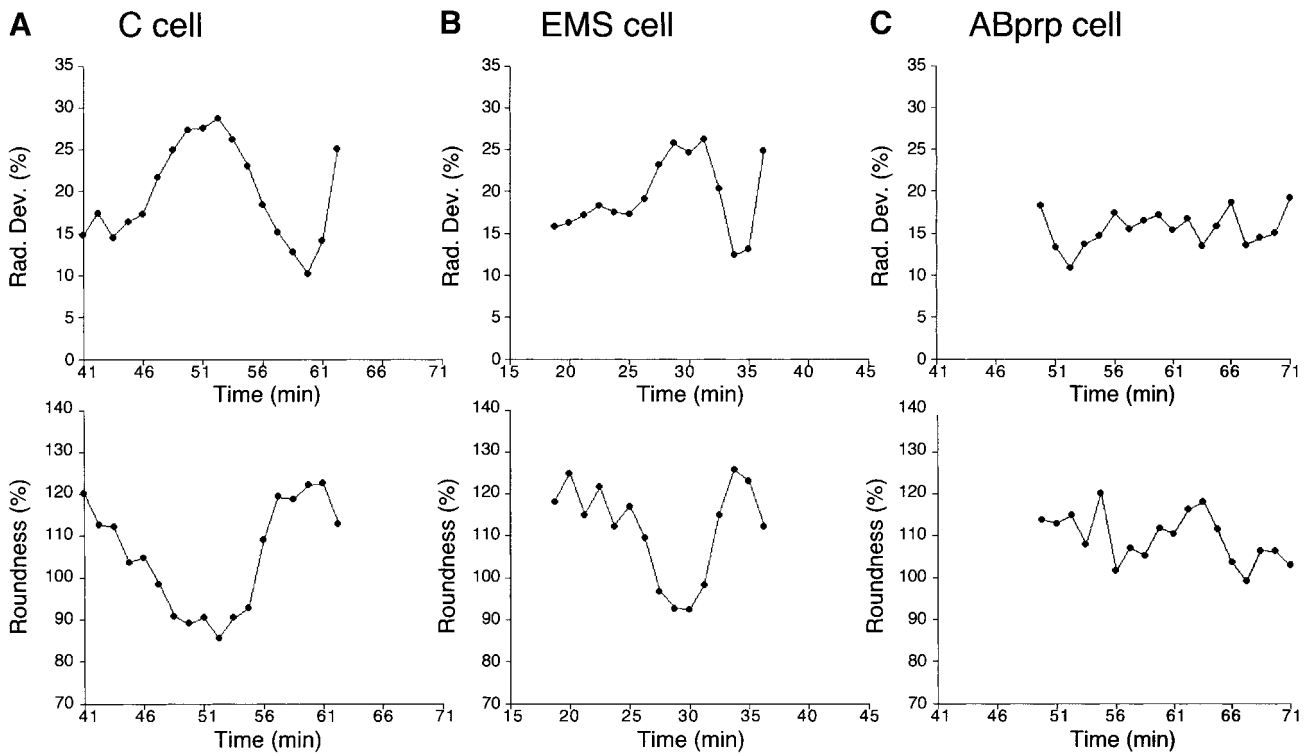

FIG. 11. 3D-DIASemb provides time plots of morphology parameters of individual cells, in this case radial deviation (Rad. Dev.) and roundness. In the case of the C (A) and EMS (B) cells, "radial deviation" increases and "roundness" decreases when these cells form extensions (see Fig. 8). In the case of the ABprp cell (C), which forms no extension, these two parameters stay relatively constant. Radial Deviation (Rad Dev) was computed to the formula Rad Dev = 100 × SD/Rad Len in which SD is standard deviation and Rad Len is radial length, according to Soll (1995). Roundness (Rnd) was computed as the efficiency of the perimeter enclosure of area according to the formula Rnd = 100 × 4Π × (Area/Perimeter^2), according to Soll (1995).

between 2000 and 2500 μm^3, with a mean (± SD) of 2300 ± 245 μm^3. After the first division, the volumes ranged between 1000 and 1650 μm^3, with a mean of 1300 ± 236 μm^3, approximately half that of the mean volume prior to division. After the second division, the volumes of the 16 progeny cells ranged between 550 and 950 μm^3, with a mean of 780 ± 136 μm^3, which was 60% of the mean volume prior to division. Both the synchrony and symmetry of the AB cell divisions were previously reported (Sulston *et al.*, 1983; Deppe, *et al.*, 1978). Previous observations of volume symmetry were qualitative in nature, while timing measurements were more quantitative, but often required analysis of multiple embryos, especially for later events. 3D-DIASemb provides quantitative time plots of these processes in single embryos. This allows the user to discriminate small quantitative differences at intervals as short as 5 s between cells of the same embryo, and small differences in embryonic events between different embryos a particularly useful tool in the analysis of mutants.

In Fig. 10B, the volumes of the C cell and its progeny are monitored through one cell division. It is clear from the plots that the C cell divided at 60 min, approximately 12 min after synchronous division of the four AB cells and approximately 10 min prior to synchronous division of the eight progeny AB cells, providing reasonably concise relative measures of the times of cleavage of different cell types. Unlike the AB cells, C cell cleavage was asymmetric. The volume of the C cell was 1750 μm^3, and the volumes of progeny cells Ca and Cp were approximately 800 and 1300 μm^3, respectively. The constancy of the volume measurements over time of Ca and Cp demonstrates that the volume difference between them is real. An analysis of a second embryo revealed a similar difference. The volumes of the progeny cells Ca and Cp were 800 and 1400 μm^3. The volume ratios of Ca to Cp in the two experiments were 0.61 and 0.57. This difference was not previously noted in the literature. In fact, C cell division was previously described as symmetric (Sulston *et al.*, 1983; Deppe *et al.*, 1978). The summed volumes of the daughter cells in the two analyzed embryos were within 20% of parent cell volume.

In Fig. 10C, the volumes of the P_3 cell and its progeny are monitored between 39 and 94 min. Cleavage was asymmetric resulting in two daughter cells with volumes of 700 and 400 μm^3. The summed volume of the P_3 daughter cells

© 2002 Elsevier Science (USA). All rights reserved.

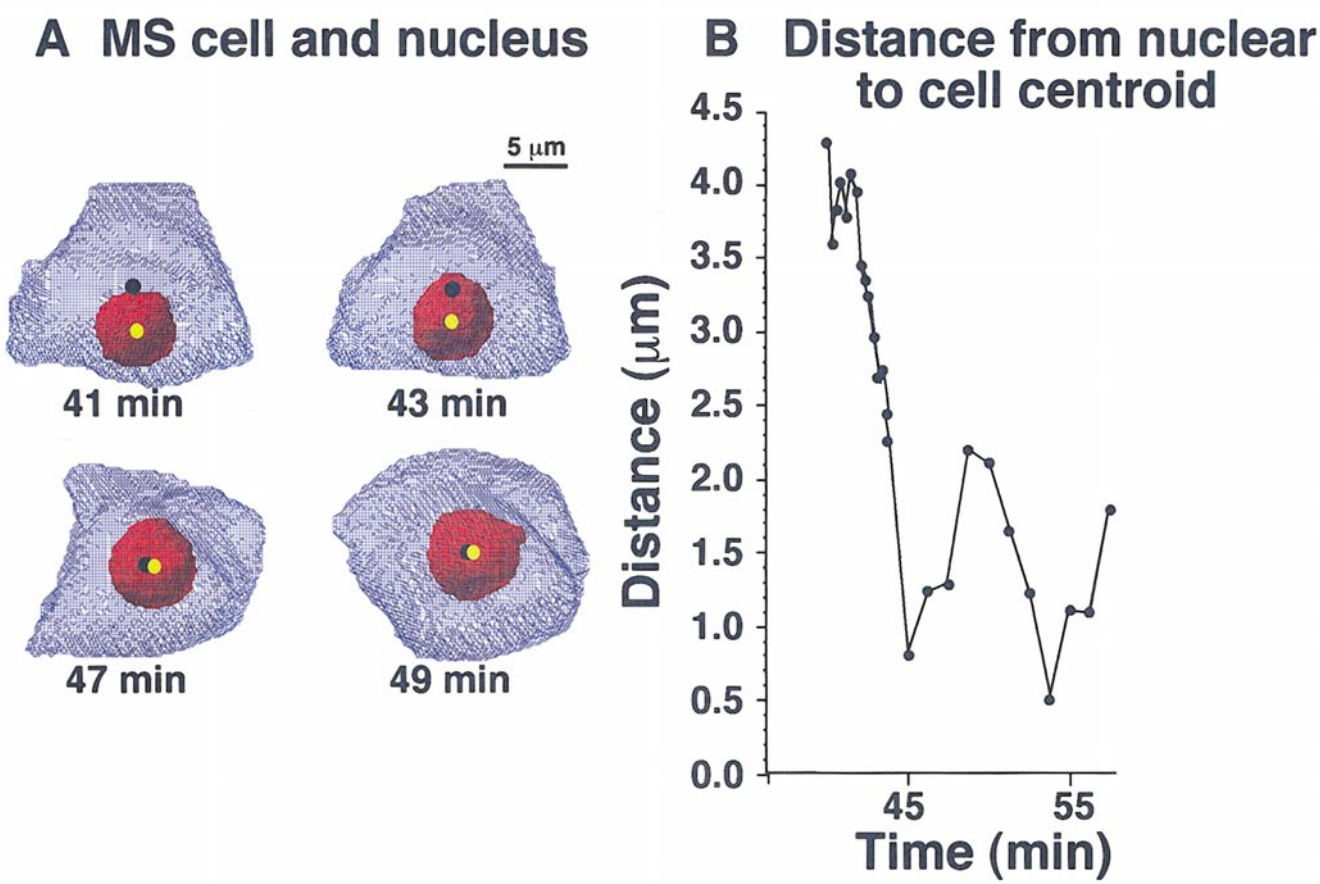

FIG. 12. 3D-DIASemb provides measures of nuclear localization within a cell. An example is presented of the MS cell, in which the nucleus is close to the membrane after birth (cleavage) and then migrates to the center of the cell. (A) Transparent reconstruction of the MS cell that includes nontransparent reconstruction of the nucleus and the cellular (black dot) and nuclear (yellow dot) centroids. (B) Time plot of the distance between the cellular and nuclear centroids.

(1100 μm^3) was within 10% of that of the mother cell (1050 μm^3). In Fig. 10D, the volume of the E cell was monitored through one division. The E cell (1700 μm^3) divided at 58 min and resulted in daughter cells of equal volume (~900 μm^3). Similarly, in Fig. 10E, the volume of the MS founder cell was monitored through two cell divisions. The MS cell divided symmetrically at 57 min and the progeny divided synchronously and symmetrically at 82 min. The asymmetry of the P_3 cell division and the symmetry of the E cell and MS cell divisions were previously observed qualitatively (Sulston *et al.*, 1983; Deppe *et al.*, 1978).

Therefore, by generating time plots of the volumes of cells and their progeny during embryogenesis, 3D-DIASemb provides a record of the relative times of cell divisions (Fig. 10F) and an assessment of the symmetry of divisions. Because the data are obtained from a single embryo, one can assess small differences in cleavage time between different cell types and progeny, and verify these differences by analyzing multiple embryos. Because the temporal resolution equals the minimum interval time between reconstructions (i.e., 5 s), one can theoretically assess differences close to that time interval.

In addition to size measurements, 3D-DIAS computes a number of shape parameters, including radial deviation and roundness. In Figs. 11A and 11B, these parameters have been computed over time for the C cell and EMS cell during the period each elongates and then rounds up again. Both cells displayed a peak in the plot of radial deviation and a valley in the plot of cell roundness at precisely the time they were observed to extend protrusions (Figs. 8A and 8B, respectively). In contrast, the same parameters remained relatively constant for an AB cell, which underwent no obvious morphological change between divisions (Fig. 11).

Nuclear behavior can also be quantitated in a variety of ways. For instance, one can compute all of the motility and dynamic morphology parameters for nuclei that are computed for cells. One can also monitor nuclear position within a cell over time. In Fig. 12A, transparent faceted

© 2002 Elsevier Science (USA). All rights reserved.

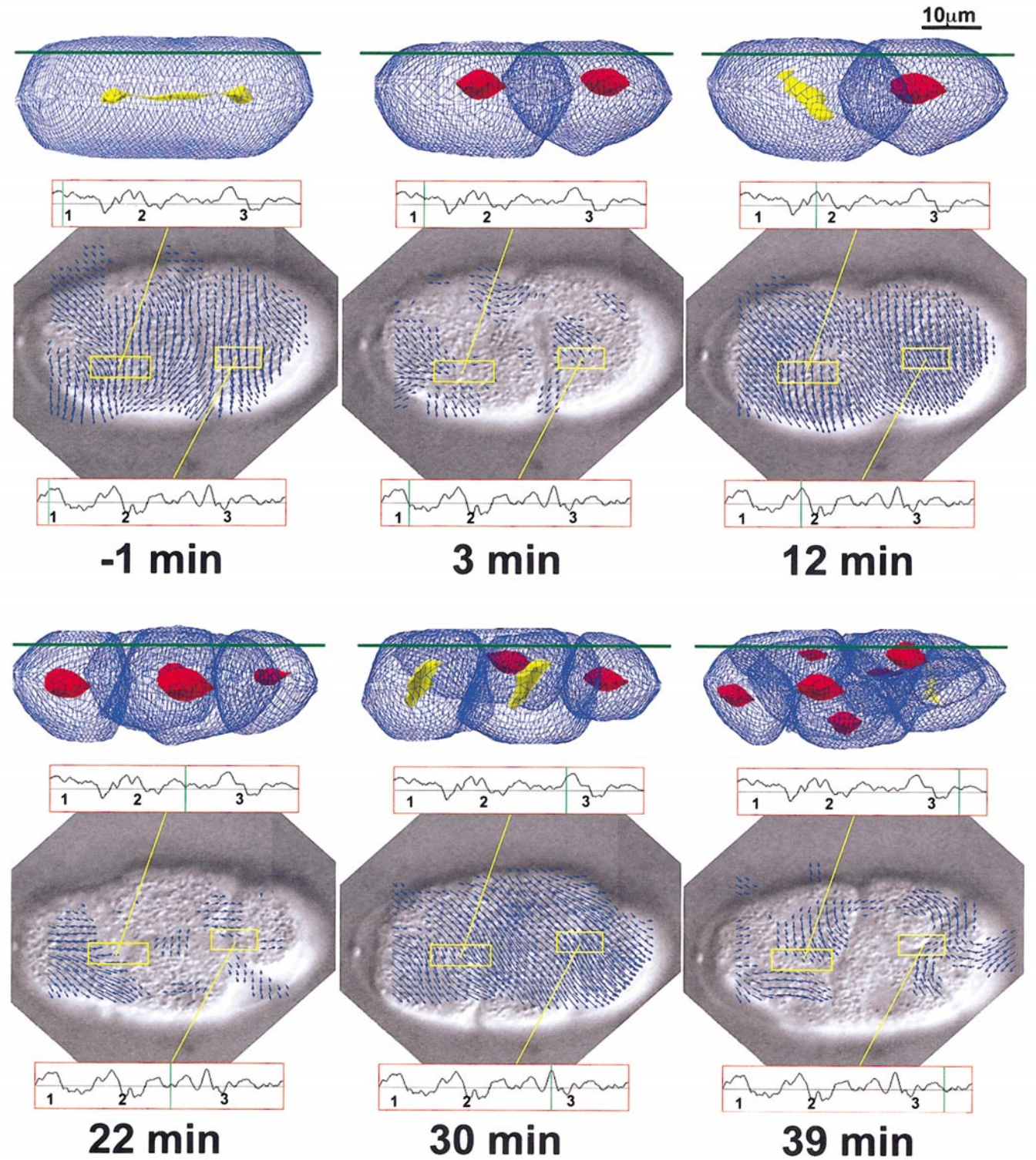

FIG. 13. 3D-DIASemb provides 2D descriptions of cytoplasmic flow at any depth in the embryo through the generation of vector flow plots of particles in the cytoplasm. In this example, the analysis spans the one-cell stage at the time of mitosis (−1 min) to seven-cell stage (39 min). At the selected time points, a side view is presented of the embryo with a green line indicating the plane of analysis, and the outlined optical section at that focal plane is presented. Vector flow plots are then superimposed on the optical section. The arrows in the vector flow plots indicate the paths of pixel movement and the lengths of the arrows are proportioned to velocity. Yellow boxes define regions of analysis in which vector lengths (velocity) are averaged. A yellow line connects these regions of analysis with the velocity plot for the entire analysis. A vertical green line denotes the exact time point of analysis along the velocity plot. Numbers 1, 2, and 3 on the graphs indicate the time at which AB, AB daughters, and AB granddaughters finish dividing, respectively.

reconstructions of the MS cell and nontransparent faceted images of its nucleus are displayed at four time points. It was observed that shortly after the birth of the MS cell at 41 min, its nucleus was positioned near the cell membrane. Over the next 8 min, however, the nucleus migrated to the center of the cell. This process was quantitated by plotting the distance between the nuclear and cell centroids as a function of time (Fig. 12B).

Vector flow plots and the analysis of cytoplasmic flow. In the development of the "Dynamic Echocardiogram Analysis System" (DEAS), which provides automatic assessments of left ventricular function using 2D motion analysis software, we created a program that analyzes ventricular wall dynamics without edge detection (Soll, 1999). Rather than assessing the movement of the computed centroid of an edge-detected, encapsulated image, this system interprets the movement of pixels within a determined window by generating vector flow plots. This method has been applied not only to the wall dynamics of the left ventricle of the human heart (Soll, 1999), but also to populations of crawling cells imaged at low magnification, in which each cell was processed as a small cluster of pixels (Escalante *et al.*, 1997). In the version of 3D-DIASemb described here, we have customized the vector flow plot program to analyze cytoplasmic particle flow in 2D at any depth in the developing embryo, using direct image reconstructions as the analyzed images. In this program, a kernel of 5×5 pixels is centered over a point of interest in video frame F and the next video frame $F + 1$. The best match, based on the mean and standard deviation of the difference in corresponding intensities, is found and an arrow (the "vector flow arrow") is constructed, connecting the original point and best match point in the next frame. Arrows are constructed and averaged over three-pixel intervals in a period of 15 s by using a Tukey window to remove noise. Arrows are drawn 10 times their actual length for visualization. The direction of the arrow represents the direction of pixel flow, and the relative length reflects speed (i.e., the longer the faster). For direct image reconstructions, a single plane of choice is analyzed over time. In Fig. 13, the plane of analysis is indicated by the green line through the image viewed from the side in the upper panel at each time point. Vector flow plots are then continuously generated at short time intervals. In Fig. 13, vector flow plots were selected for presentation at -1, 3, 12, 22, 30, and 39 min after the first mitosis. Two regions indicated by yellow boxes were then monitored over time. The average velocity of pixels in the two regions was continuously graphed above and below the vector flow plot images. Each plot is connected to the region of analysis by a yellow line. The vertical green line along each graph defines the time point along the velocity plot. Peaks in velocity were observed in the one-, two-, and four-cell embryos just prior to division of P_o, AB, and ABa/ABp, respectively. These peaks correlated with the rapid circular rotation of cytoplasmic particles in unison in the dorsal/ventral direction. A similar process was previously described in the four-cell embryo (Sulston *et al.*, 1983), but not in the one- and two-cell embryos, as reported here. These rotations were observed in multiple embryos, including one that was not under pressure from the coverslip. These data display the power of this tool for the analysis of movement within the embryo at any time or level. Because cytoplasmic flow includes circular rotation in the *z* axis, the 2D analysis provided by these vector flow plots provides useful but incomplete descriptions. Therefore, algorithms are now being written in 3D-DIASemb to generate 3D vector flow plots.

DISCUSSION

Computer assisted motion analysis systems based on edge detection hardware and software have been used for the past 16 years to analyze how cells crawl (Soll, 1995). These systems at first employed real-time contour digitizers for automatic 2D edge detection, and developed from centroid-based systems restricted to computing motility parameters to dynamic morphology systems that also included measurements of the changing cell contour (Soll, 1995; Soll and Voss 1998). After 1990, these systems employed frame grabbers and software for edge detection, thus eliminating contour digitizers (Soll, 1995). In the early 1990s, the first 3D reconstruction and motion analysis systems were introduced (Soll, 1995; Soll and Voss 1998; Wessels *et al.*, 1998), which involved manual outlining or performed automatic edge detection in optical sections, converted the identified perimeters to β-spline models, stacked the perimeters in the *z* axis, and then generated 3D faceted images of a cells surface at intervals as short as 1 s. When strung together in a movie format, one could watch for the first time a crawling cell in 3D at any desired angle through a stereo workstation. More importantly, because the dynamic 3D image was now a mathematical model, one could quantitate over 100 parameters of motility and dynamic morphology (Soll, 1995; Soll and Voss 1998). In 1998, these systems were expanded to include the reconstruction and motion analysis of the cell nucleus and pseudopod (Wessels *et al.*, 1998) and intracellular particles (Wessels *et al.*, 2000a).

We have used this 3D single cell technology (3D-DIAS) as the basis for developing 3D-DIASemb, which includes software that can handle the increase in individual components (i.e., cells and nuclei). Each optical section of an embryo includes an increasing number of cells and nuclei, each requiring independent trace slots for reconstruction. This software separates and reconstructs individual components, then melds them together to generate a complex 3D β-spline model of the developing embryo that can be selectively dissected and motion analyzed. We have developed software that allows one to view only cell surfaces, only nuclei, only a particular cell lineage, only a particular nuclear lineage, or only a group of associated cells. Because each component represents a β-spline model, one can quantitate motility parameters from the 3D track of its

© 2002 Elsevier Science (USA). All rights reserved.

centroid and dynamic morphology parameters from the changes in contour. By dissecting components from the model, such as the cells involved in ingression during gastrulation, one can begin to describe in 4D embryogenic phenomena at the cellular level.

We have used *C. elegans* embryogenesis as the experimental system for the initial development of 3D-DIASemb because it includes a very limited number of cells, undergoes mosaic development, with lineages carefully defined in the literature (Sulston *et al.*, 1983; Sulston and Horvitz, 1977; Deppe *et al.*, 1978; Kimble and Hirsh, 1979), and has been the object of intense mutational analysis (e.g., Brenner, 1974; Cassada *et al.*, 1981; O'Connell *et al.*, 1998; Ahnn and Fire, 1994; Chanal and Labouesse, 1997). Because of low cell number and a relatively transparent cytoplasm, we have been able to use differential interference contrast microscopy to reconstruct and motion-analyze development through the 28-cell stage, and in the near future will attempt to reconstruct all of *C. elegans* embryogenesis. Because of its advantages as an experimental system, methods have been developed by several groups for optical sectioning, image storage, processing, and presentation (Thomas and White, 1998; Schnabel *et al.*, 1997; Schierenberg *et al.*, 1986; Fire, 1994; Burglin, 2000; Mohler and White, 1998a,b). Software has been developed for manually recording the position of nuclei and cells in order to monitor cell division, cell position, cell–cell interactions, and lineages (Schnabel *et al.*, 1997). These systems have been particularly effective in following lineages. However, none of these systems include software for edge detection, the genesis of 3D β-spline models of cell and nuclear shape, or motion analysis software comparable to that now in place in 3D-DIASemb. The value of 3D-DIASemb in the case of *C. elegans* will ultimately be in the analysis of mutants. 3D-DIASemb provides an extraordinary level of 4D phenotypic resolution for comparing wild-type and mutant embryogenesis. Once the database for wild-type embryogenesis is established, researchers will be able to analyze mutant embryos beginning at the stage they believe the first defects arise, and compare their data set with a detailed wild-type data set. The value of such comparisons is evident in the use of 2D- and/or 3D-DIAS for analysis of mutant larval behavior in *Drosophila* (Wang *et al.*, 1997, 2001) and *Caenorhabditis* (de Bono and Bargmann, 1998), white blood cell behavior (Shutt *et al.*, 1998, 2000), cancer cell behavior (Farina *et al.*, 1998; Bailly *et al.*, 1998), fibroblast motility (Bear *et al.*, 2000), epidermal growth factor-induced motility (Shiraha *et al.*, 1999), neural adhesion and growth cone motility (Kim and Wu, 1996), the role of cytoskeleton in mitosis (Wong *et al.*, 2000), and the roles of specific cytoskeletal and regulatory molecules in *Dictyostelium* motility and chemotaxis (Wessels and Soll, 1998; Shutt *et al.*, 1995; Wessels *et al.*, 2000a,b; Tuxworth *et al.*, 2001; Chung and Firtel, 1999; Chung *et al.*, 2001; Shelden and Knecht, 1996).

Although 3D-DIASemb has been developed with *C. elegans* as the experimental system, our goal is to generalize the program so that it can be applied to sea urchin, *Drosophila melanogaster*, zebrafish, and early baboon embryogenesis. An analysis of early zebrafish development using 3D-DIASemb has already been initiated, and customized software for this system is now being added to 3D-DIASemb. It should be noted that 3D-DIASemb will also be expanded for use in reconstructing and motion-analyzing tissue and organ development, and the behavior of single cells in tissue.

We have described here the first prototype of 3D-DIASemb. Although functional, it is incomplete. First, we are working intensely on programs for automatically outlining the edges of cells in optical sections of a developing embryo taken through DIC optics, thus eliminating all manual tracing. A program has already been developed for the automatic edge detection of nuclear perimeters. Second, we are optimizing software that automatically detects the edges of cells in confocal optical sections of developing embryos vitally stained with fluorescent dyes. Third, we are in the process of transferring 3D-DIASemb to a new JAVA-based DIAS 4.0 platform that will facilitate reconstruction and motion analysis. Finally, we are in the process of developing motion analysis software for describing and quantitating parameters specific to embryogenesis, including ones based on cell–cell interactions, the spatial and temporal dynamics of groups of cells, and the development of cell lineages. This system provides a new method for reconstructing and motion analyzing in 4D every cell and nucleus in a developing embryo. Its power will be in identifying changes and defects in embryogenesis caused by drugs, environmental perturbations, and mutations. 3D-DIASemb system, as described here, is now available for use through collaboration in the W. M. Keck Dynamic Image Analysis Facility at the University of Iowa. The dynamic reconstructions can be viewed and downloaded from the W. M. Keck Dynamic Image Analysis Facility Web site (http://keck.biology.uiowa.edu).

ACKNOWLEDGMENTS

We thank Dr. Karla Daniels for help in developing some of the figures. The development of 3D-DIASemb was supported in part by National Institutes of Health Grant HD-18577 and by the W. M. Keck Foundation. P.H. was supported by a postdoctoral fellowship provided by the American Cancer Society (Grant PF-01-110-01-CSM).

REFERENCES

Ahnn, J., and Fire, A. (1994). A screen for genetic loci required for body-wall muscle development during embryogenesis in *Caenorhabditis elegans*. *Genetics* **137,** 483–498.

Bailly, M., Yan, L., Whitesides, G. M., Condeelis, J. S., and Segall, J. E. (1998). Regulation of protrusion shape and adhesion to the substratum during chemotactic responses of mammalian carcinoma cells. *Exp. Cell Res.* **241,** 285–299.

© 2002 Elsevier Science (USA). All rights reserved.

Barsky, B. A. (1988). "Computer Graphics and Geometric Modeling Using Beta-Splines." Springer-Verlag, Berlin.

Bear, J. E., Loureiro, J. J., Libova, I., Fassler, R., Wehland, J., and Gertler, F. B. (2000). Negative regulation of fibroblast motility by Ena/VASP proteins. *Cell* **101,** 717–728.

Brenner, S. (1974). The genetics of *Caenorhabditis elegans*. *Genetics* **77,** 71–94.

Burglin, T. R. (2000). A two-channel four-dimensional image recording and viewing system with automatic drift correction. *J. Microsc.* **200,** 75–80.

Cassada, R., Isnenghi, E., Culotti, M., and von Ehrenstein, G. (1981). Genetic analysis of temperature-sensitive embryogenesis mutants in *Caenorhabditis elegans*. *Dev. Biol.* **84,** 193–205.

Chanal, P., and Labouesse, M. (1997). A screen for genetic loci required for hypodermal cell and glial-like cell development during *Caenorhabditis elegans* embryogenesis. *Genetics* **146,** 207–226.

Chung, C. Y., and Firtel, R. A. (1999). PAKa, a putative PAK family member is required for cytokinesis and the regulation of the cytoskeleton in *Dictyostelium discoideum* cells. *J. Cell Biol.* **147,** 559–576.

Chung, C. Y., Potikyan, G., and Firtel, R. A. (2001). Control of cell polarity and chemotaxis by Akt/PKB and P13 kinase through the regulation of PAKa. *Mol. Cell.* **7,** 937–947.

de Bono, M., and Bargmann, C. I. (1998). Natural variation in a neuropeptide Y receptor homolog modifies social behavior and food response in *C. elegans*. *Cell* **94,** 679–689.

Deppe, U., Schierenberg, E., Cole, T., Krieg, C., Schmitt, D., Yoder, B., and von Ehrenstein, G. (1978). Cell lineages of the embryo of the nematode *Caenorhabditis elegans*. *Proc. Natl. Acad. Sci. USA* **75,** 376–380.

Escalante, R., Wessels, D., Soll, D. R., and Loomis, W. F. (1997). Chemotaxis to cAMP and slug migration in *Dictyostelium* both depend on MigA, a BTB protein. *Mol. Biol. Cell* **8,** 1763–1775.

Farina, K. L., Wyckoff, J. B., Rivera, J., Lee, H., Segall, J. E., Condeelis, J. S., and Jones, J. G. (1998). Cell motility of tumor cells visualized in living intact primary tumors using green fluorescent protein. *Cancer Res.* **58,** 2528–2532.

Fire, A. (1994). A four-dimensional digital image archiving system for cell lineage tracing and retrospective embryology. *Comput. Appl. Biosci.* **10,** 443–447.

Kim, Y. T, and Wu, C. F. (1996). Reduced growth cone motility in cultured neurons from *Drosophila* memory mutants with a defective cAMP cascade. *J. Neurosci.* **16,** 5593–5602.

Kimble, J., and Hirsh D. (1979). The postembryonic cell lineages of the hermaphrodite and male gonads in *Caenorhabditis elegans*. *Dev. Biol.* **70,** 396–417.

Mohler, W. A., and White, J. G. (1998a). Stereo-4-D reconstruction and animation from living fluorescent specimens. *Biotechniques* **24,** 1006–1010, 1012.

Mohler, W. A., and White, J. G. (1998b). Multiphoton laser scanning microscopy for four-dimensional analysis of *Caenorhabditis elegans* embryonic development. *Optics Express* **3,** 325–331.

Murray, J., Vawter-Hugart, H., Voss, E., and Soll, D. R. (1992). Three-dimensional motility cycle in leukocytes. *Cell Motil. Cytoskeleton* **22,** 211–223.

O'Connell, K. F., Leys, C. M., and White, J. G. (1998). A genetic screen for temperature-sensitive cell-division mutants of *Caenorhabditis elegans*. *Genetics* **149,** 1303–1321.

Saloman, D. (1998). "Data Compression." Springer, New York.

Schierenberg, E., Cole, T., Carlson, C., and Sidio, W. (1986). Computer-aided three-dimensional reconstruction of nematode embryos from EM serial sections. *Exp. Cell Res.* **166,** 247–52.

Schnabel, R., Hutter, H., Moerman, D., and Schnabel, H. (1997). Assessing normal embryogenesis in *Caenorhabditis elegans* using a 4D microscope: variability of development and regional specification. *Dev. Biol.* **184,** 234–265.

Shelden, E., and Knecht, D. A. (1996). *Dictyostelium* cell shape generation requires myosin II. *Cell Motil. Cytoskeleton* **35,** 59–67.

Shiraha, H., Glading, A., Gupta, K., and Wells, A. (1999). IP-10 inhibits epidermal growth factor-induced motility by decreasing epidermal growth factor receptor-mediated calpain activity. *J. Cell Biol.* **146,** 243–254.

Shutt, D., Wessels, D., Wagenknecht, K., Chandrasekhar, B., Hitt, A., Luna, E. J., and Soll, D. R. (1995). Ponticulin plays a role in the positional stabilization of pseudopods. *J. Cell Biol.* **131,** 1495–1506.

Shutt, D., Jenkins, L. M., Carolan, E. J., Stapleton, J., Daniels, K. J., Kennedy, R. C., and Soll, D. R. (1998). T cell syncytia induced by HIV release T cell chemoattractants: Demonstration with a newly developed single cell chemotaxis. *J. Cell Sci.* **111,** 99–109.

Shutt, D. C., Daniels, K. J., Carolan, E. J., Hill, A. C., and Soll, D. R. (2000). Changes in the motility, morphology, and F-actin architecture of human dendritic cells in an in vitro model of dendritic cell development. *Cell Motil. Cytoskeleton* **46,** 200–221.

Soll, D. R. (1995). The use of computers in understanding how animal cells crawl. *Int. Rev. Cytol.* **163,** 43–104.

Soll, D. R., and Voss, E. (1998). Two and three dimensional computer systems for analyzing how cells crawl. In "Motion Analysis of Living Cells" (D. R. Soll and D. Wessels, Eds.), pp. 25–52. John Wiley, Inc., New York.

Soll, D. R. (1999). Computer-assisted three-dimensional reconstruction and motion analysis of living, crawling cells. *Comput. Med. Imaging Graph.* **23,** 3–14.

Soll, D. R., Voss, E., Johnson, O., and Wessels, D. J. (2000). Three-dimensional reconstruction and motion analysis of living crawling cells. *Scanning* **22,** 249–257.

Stites, J., Wessels, D., Uhl, A., Egelhoff, T. E., Shutt, D., and Soll, D. R. (1998). Phosphorylation of the *Dictyostelium* myosin II heavy chain is necessary for maintaining cellular polarity and suppressing turning during chemotaxis. *Cell Motil. Cytoskeleton* **39,** 31–51.

Sulston, J. E., and Horvitz, H. R. (1977). Post-embryonic cell lineages of the nematode *Caenorhabditis elegans*. *Dev. Biol.* **56,** 110–156.

Sulston, J. E., Schierenberg, E., White, J. G., and Thomson, J. N. (1983). The embryonic cell lineage of the nematode *Caenorhabditis elegans*. *Dev. Biol.* **100,** 64–119.

Thomas, C. F., and White, J. G. (1998). Four-dimensional imaging: the exploration of space and time. *Trends Biotechnol.* **16,** 175–182.

Tuxworth, R., Weber, I., Wessels, D., Addicks, G. C., Soll, D. R., Gerisch, G., and Titus, M. (2001). A role for myosin VII in dynamic cell adhesion. *Curr. Biol.* **11,** 1–20.

Wang, J., Sylwester, W., Reed, D., Wu, D-A. J., Soll, D. R., and Wu, C-F. (1997). Morphometric description of the wandering behavior in *Drosophila* larvae: Aberrant locomotion in Na+ and K+ channel mutants revealed by computer-assisted motion analysis. *J. Neurogenet.* **11,** 231–254.

Wang, J. W., Soll, D. R., and Wu, C.-F. (2002). Morphometric description of the wandering behavior in *Drosophila* larvae: A

© 2002 Elsevier Science (USA). All rights reserved.

phenotypic analysis of K+ channel mutants. *J. Neurogenet.*, in press.

Watt, A. (1993). "3D Computer Graphics," Chapters 12 and 14. Addison-Wesley, New York.

Wessels, D., Voss, E., Von Bergen, N., Burns, R., Stites, J., and Soll, D. R. (1998). A computer-assisted system for reconstructing and interpreting the dynamic three-dimensional relationships of the outer surface, nucleus and pseudopods of crawling cells. *Cell Motil. Cytoskeleton* **41,** 225–246.

Wessels, D., and Soll, D. R. (1998). Computer-assisted characterization of the behavioral defects of cytoskeletal mutants of *Dictyostelium discoideum*. In "Motion Analysis of Living Cells" (D. R. Soll and D. Wessels, Eds.), pp. 101–140. John Wiley, Inc., New York.

Wessels, D., Reynolds, J., Johnson, O., Voss, E., Burns, R., Daniels, K., Garrard, E., O'Hallaran, T., and Soll, D. R. (2000a). Clathrin plays a novel role in the regulation of cell polarity, pseudopod formation, uropod stability and motility in *Dictyostelium*. *J. Cell Sci.* **113,** 26–36.

Wessels, D., Zhang, H., Reynolds, J., Daniels, K., Heid, P., Liu, S., Kuspa, A., Shaulsky, G., Loomis, W. F., and Soll, D. R. (2000b). The internal phosphodiesterase *RegA* is essential for the suppression of lateral pseudopods during *Dictyostelium* chemotaxis. *Mol. Biol. Cell* **11,** 2803–2820.

Wong, K., Wessels, D., Krob, S., Matveia, A. R., Lin, J. L., Soll, D. R., and Lin, J. J. (2000). Forced expression of dominant-negative chimaric tropomyosin causes abnormal motile behavior during cell division. *Cell Motil. Cytoskeleton* **45,** 121–132.

Received for publication January 10, 2002
Revised February 14, 2002
Accepted February 14, 2002
Published online April 16, 2002

© 2002 Elsevier Science (USA). All rights reserved.